

Hyperthermia adds to trabectedin effectiveness and thermal enhancement is associated with BRCA2 degradation and impairment of DNA homologous recombination repair

Dominique Harnicek*², Eric Kampmann#*¹, Kirsten Lauber³, Roman Henkel³, Ana Sofia Cardoso Martins¹, Yang Guo⁵, Claus Belka³, Simone Mörtl⁴, Eike Gallmeier⁶, Roland Kanaar⁷, Ulrich Mansmann⁸, Tomas Hucl⁹, Lars H. Lindner¹, Wolfgang Hiddemann¹, Rolf D. Issels¹

*Authors contributed equally

#Corresponding author

¹Department of Medicine III, University Hospital Grosshadern, University of Munich, Munich, Germany

²Hämatologikum of the Helmholtz Center Munich, German Research Center for Environmental Health, Munich, Germany

³Department of Radiation Oncology, University Hospital Grosshadern, University of Munich, Munich, Germany

⁴Institute of Radiation Biology Helmholtz Zentrum München, German Research Center for Environmental Health, Munich, Germany

⁵Department of Medicine II, University Hospital Grosshadern, University of Munich, Munich, Germany

⁶Department of Internal Medicine, Philipps University of Marburg, Marburg, Germany

⁷Department of Genetics, Cancer Genomics Netherlands, Department of Radiation Oncology, Erasmus Medical Center, Rotterdam, Netherlands

⁸Institute of Medical Informatics, Biostatistics, and Epidemiology, Campus Grosshadern, University of Munich, Munich, Germany

⁹Department of Gastroenterology and Hepatology, Institute for Clinical and Experimental Medicine, Prague, Czech Republic

All authors declare that there are no personal or financial conflicts of interest.

Corresponding author:

Eric Kampmann, M.D., Department of Medicine III, University of Munich, Munich, Germany

Phone: +49 - 89 - 44007 - 4768

Fax: +49 - 89 - 44007 - 4776

E-mail: eric.kampmann@med.uni-muenchen.de

Postal address: Medizinische Klinik III, Klinikum Grosshadern
Marchioninstr. 15
D-81377 München
Germany

This article has been accepted for publication and undergone full peer review but has not been through the copyediting, typesetting, pagination and proofreading process which may lead to differences between this version and the Version of Record. Please cite this article as an 'Accepted Article', doi: 10.1002/ijc.30070

Affiliations:

Dominique Harnicek: Hämatologikum of the Helmholtz Center Munich, German Research Center for Environmental Health, Munich, Germany; dominique.harnicek@helmholtz-muenchen.de

Eric Kampmann: Department of Medicine III, University Hospital Grosshadern, University of Munich, Munich, Germany; eric.Kampmann@med.uni-muenchen.de

Kirsten Lauber: Department of Radiation Oncology, University Hospital Grosshadern, University of Munich, Munich, Germany; kirsten.lauber@med.uni-muenchen.de

Roman Hennel: Department of Radiation Oncology, University Hospital Grosshadern, University of Munich, Munich, Germany; roman.hennel@med.uni-muenchen.de

Ana Sofia Cardoso Martins: Hämatologikum of the Helmholtz Center Munich, German Research Center for Environmental Health, Munich, Germany; anasofiacm.martins@gmail.com

Yang Guo: Department of Medicine II, University Hospital Grosshadern, University of Munich, Munich, Germany; guoyang2010@aol.com

Claus Belka: Department of Radiation Oncology, University Hospital Grosshadern, University of Munich, Munich, Germany; claus.belka@med.uni-muenchen.de

Simone Mörtl: Institute of Radioation Biology, Helmholtz Zentrum Muenchen, German Research Center for Environmental Health, Munich, Germany; moertl@helmholtz-muenchen.de

Eike Gallmeier: Department of Internal Medicine, Philipps University of Marburg, Marburg, Germany; gallmeie@med.uni-marburg.de

Roland Kanaar: Department of Genetics, Cancer Genomics Netherlands, Department of Radiation Oncology, Erasmus Medical Center, Rotterdam, Netherlands; r.kanaar@erasmusmc.nl

Ulrich Mansmann: Institute of Medical Informatics, Biostatistics, and Epidemiology, Campus Grosshadern, University of Munich, Munich, Germany; mansmann@ibe.med.uni-muenchen.de

Tomas Hucl: Department of Gastroenterology and Hepatology, Institute for Clinical and Experimental Medicine, Prague, Czech Republic; tohu@medicon.cz

Lars H. Lindner: Department of Medicine III, University Hospital Grosshadern, University of Munich, Munich, Germany; lars.lindner@med.uni-muenchen.de

Wolfgang Hiddemann: Department of Medicine III, University Hospital Grosshadern, University of Munich, Munich, Germany; wolfgang.hiddemann@med.uni-muenchen.de

Rolf D. Issels: Department of Medicine III, University Hospital Grosshadern, University of Munich, Munich, Germany and Hämatologikum of the Helmholtz Center Munich, German Research Center for Environmental Health, Munich, Germany; rolf.issels@med.uni-muenchen.de

Key Words

Sarcoma; Trabectedin; Hyperthermia; DNA-repair

Abbreviations

DSB – DNA double-strand breaks, HRR – homologous recombination repair, NER – nucleotide excision repair, PFS – progression free survival, OS – overall survival, PBMC – peripheral blood mononuclear cell

What's new

Hyperthermia is shown to enhance the antitumor effectiveness of the drug trabectedin. Combination treatment significantly increases the amount of DNA damage accompanied by enhanced cell cycle arrest, induction of apoptosis or senescence and reduced clonogenic survival. Hyperthermia impairs homologous recombination repair of DNA double-strand breaks mainly by BRCA2 degradation and disrupted recruitment of recombinase RAD51 to the DNA repair foci. The amount of repair foci positive PBMCs from patients might be a potential surrogate marker.

Abstract

The tetrahydroisoquinoline trabectedin is a marine compound with approved activity against human soft-tissue sarcoma. It exerts anti-proliferative activity mainly by specific binding to the DNA and inducing DNA double-strand breaks (DSB). Since homologous recombination repair (HRR) deficient tumors are more susceptible to trabectedin, hyperthermia mediated on-demand induction of HRR deficiency represents a novel and promising strategy to boost trabectedin treatment.

For the first time, we demonstrate enhancement of trabectedin effectiveness in human sarcoma cell lines by heat and characterize cellular events and molecular mechanisms related to heat-induced effects. Hyperthermic temperatures (41.8°C or 43°C) enhanced significantly trabectedin-related clonogenic cell death and G2/M cell cycle arrest followed by cell type dependent induction of apoptosis or senescence. Heat combination increased accumulation of γ H2AX foci as key marker of DSBs. Expression of BRCA2 protein, an integral protein of the HRR machinery, was significantly decreased by heat. Consequently, recruitment of downstream RAD51 to γ H2AX positive repair foci was almost abolished indicating relevant impairment of HRR by heat. Accordingly, enhancement of trabectedin effectiveness was significantly augmented in BRCA2-proficient cells by hyperthermia and alleviated in BRCA2 knockout or siRNA transfected BRCA2 knockdown cells. In peripheral blood mononuclear cells isolated from sarcoma patients, increased numbers of nuclear γ H2AX foci were detected after systemic treatment with trabectedin and hyperthermia of the tumor region.

The findings establish BRCA2 degradation by heat as a key factor for a novel treatment strategy that allows targeted chemosensitization to trabectedin and other DNA damaging antitumor drugs by on-demand induction of HRR deficiency.

Introduction

Trabectedin (Yondelis®) is a DNA-intercalating anticancer drug originally isolated from the sea squirt *Ecteinascidia turbinata*. The drug is established for the treatment of advanced soft-tissue sarcoma after failure of anthracyclines and ifosfamide as well as for the treatment of platinum-sensitive ovarian carcinoma in combination with liposomal doxorubicin. In sarcoma, trabectedin usually induces high rates of tumor growth arrest. In a worldwide-expanded access program investigating 1895 patients, stable disease was reported in 43% and overall survival was 11.9 months. Unfortunately, treatment response with relevant tumor shrinkage was only seen in 5% (1). Given the worse prognosis of advanced sarcoma, there is urgent need to improve treatment. Enhancing anti-tumor efficacy of trabectedin by a local treatment seems to be a promising strategy.

Trabectedin binds covalently to the minor groove of the DNA double helix inhibiting trans-activated transcription and stalling DNA replication forks. These actions trigger a cascade of events that lead to the generation of DNA double-strand breaks (DSB), G2/M cell cycle arrest and apoptosis (2). The endonuclease ERCC5 is a key-protein of the DNA nucleotide excision repair (NER). Binding of ERCC5 (alias xeroderma pigmentosum group G [XPG]) and further NER proteins to trabectedin-DNA-adducts are important steps for the generation of DSBs. Accordingly, effectiveness of trabectedin depends on an intact NER, but is remarkably enhanced in tumors with deficiencies in the DNA homologous recombination repair (HRR), which represents the main repair pathway for DSBs in late S and G2 phase (3). Consistently, the expressions of genes and single nucleotide polymorphisms (SNPs) involved in both, the NER and HRR, have been demonstrated as differential predictive factors for treatment response and survival in patients treated with trabectedin (4–6). Additionally, trabectedin – at therapeutic concentrations – has immunomodulatory properties. It selectively targets mononuclear cells including monocytes and tumor-associated macrophages and down-regulates the production of proinflammatory mediators, which induces changes in the tumor microenvironment also contributing to the antitumor activity (7–9).

In the last years, regional hyperthermia inducing controlled temperature elevation in locally advanced tumors applied together with radiotherapy or chemotherapy has entered the clinical field of oncology (10). For high-risk soft-tissue sarcoma patients, in one large randomized, multicentric phase III trial, regional hyperthermia combined with neoadjuvant chemotherapy as first-line treatment improved response rate, local progression-free and disease-free survival (11). The cytotoxic effects of hyperthermia and the enhancement of drug effectiveness for several anticancer agents by heat exposure at clinically relevant temperatures (range: 40°C to 43°C) *in vitro* and *in vivo* are reviewed by Hildebrandt et al. (2002) and Issels (2008). Interestingly, enhanced DNA damage and DSB formation by dysfunction of heat-labile repair proteins and inhibition of HRR were described in the context of hyperthermia (14–17).

At an early stage of the DNA damage response, multiple γ H2AX molecules surrounding the DSB sites are generated by phosphorylation of the histone H2AX on serine 139. Resulting γ H2AX foci are considered as a suitable marker for DSBs (18–20). More recently, for radiation induced DSBs, it has been shown that repair is impaired by hyperthermia due to heat-induced BRCA2 degradation (21). BRCA2 is a tumor suppressor, which is essential for genomic stability and indispensable for the HRR. With its carboxyl terminus, BRCA2 binds to the recombinase RAD51 and controls its DNA-binding ability as well as its localization at the DSBs. After recruitment to the site of DNA damage, RAD51 forms helical nucleoprotein filaments and initiates DSB repair (22,23).

We suggest that hyperthermia enhances the antiproliferative effects of trabectedin at clinically relevant temperatures (41.8°C – 43°C). Adding heat as a strategy that allows on-demand induction of HRR deficiency restricted to the tumor area may lead to an innovative clinical application of trabectedin and other DNA damaging antitumor drugs with an underlying molecular mechanisms we designate targeted chemosensitization.

Materials and Methods

Cell lines and treatments

Human sarcoma cell lines U2OS (osteosarcoma), SW872 (liposarcoma), SW982 (synovial sarcoma), RD-ES (Ewing sarcoma) and SKUT-1 (leiomyosarcoma) and a human colorectal carcinoma cell line (DLD1) were used. SW872 and SW982 were obtained from Cell Line Service (CLS), RD-ES and SKUT-1 from the American Type Culture Collection (ATCC). U2OS were kindly provided by R. Kanaar and DLD1 cells (parental and *BRCA2*^{-/-}) by E. Gallmeier. Culture media were DMEM plus 5% fetal calf serum (FCS) for SW872 and SW982, DMEM plus 10% FCS for U2OS and additionally with 1% penicillin/streptomycin for DLD1, Eagle's MEM plus 10% FCS, 1% non-essential amino acids, 1% sodium-pyruvate, 2 mmol/l L-glutamine for RD-ES and SKUT-1. Trabectedin was supplied by the Pharmacy, University of Munich, and stored in aliquots at concentrations of 590 nmol/l and 5.9 μ mol/l at -80°C. For experiments, exponentially growing cells in 6- or 12-well-plates cultivated at 37°C in a humidified incubator (5% CO₂) for an attachment period of 16-24 hrs were treated with trabectedin with/without hyperthermia as indicated. Trabectedin was applied for 180 min and subsequently removed by change of medium. Hyperthermia was performed for 90 min in preheated incubators with parallel sham-treatments at 37°C for 90 min since this treatment mimics best the temperature curve achieved during clinical application also lasting 90 min (Fig. S1). Sequential treatments were performed without any delay (< 10 min).

Clonogenic assays

Cells were cultivated for 7-14 days, colonies were fixed, stained with crystal violet and colonies (\geq 50 cells) were counted (24).

Cell cycle kinetics

Cells were collected and 150 μ l Nicoletti-staining solution (0.1% trisodium citrate dehydrate, 0.1% Triton X-100, 50 μ g/ml propidium iodide in ddH₂O) was added. FACS analysis was performed with a BD Accuri C6 Cytometer (BD Biosciences). By the use of BD Accuri C6 software, cell cycle distributions were analyzed and DNA histograms were performed representing cells in G1-, S- and G2/M-phase and apoptotic cells being represented by the sub G1 population.

Caspase-activity assay

Cells were collected and stored as pellets at -80°C . Whole cell protein lysates were prepared in Caspase lysis buffer (20 mM HEPES (pH 7.4), 84 mM KCl, 10 mM MgCl_2 , 0.2 mM EDTA, 0.2 mM EGTA, 0.5% NP40, supplemented with 1 mM PMSF, 1 mM DTT, 1 $\mu\text{g/ml}$ leupeptin, 1 $\mu\text{g/ml}$ pepstatin and 5 $\mu\text{g/ml}$ aprotinin) and protein concentration was determined (BCA Protein Assay Kit, Pierce). For DEVDase measurement, 20 μg of the protein was transferred in quadruplicates into 96-well plates and filled up to 100 μl with Caspase lysis buffer (without PMSF, DTT, leupeptin, pepstatin and aprotinin). Subsequently, 2x DEVDase reaction buffer (out of 10x DEVDase reaction buffer: 375 mM HEPES-Na [pH 7.4], 750 mM NaCl, 75% Saccharose, 0.75% CHAPS) supplemented with 50 mM DEVD-AMC peptide (Bachem) was added and caspase-activity was measured in a microplate reader (Synergy Mx, BioTeK) by determining kinetics of AMC-fluorescence due to DEVD-cleavage.

Senescence-associated β -galactosidase activity assay

β -Galactosidase is a marker of senescent cells (25) which can be measured by conversion of the fluorogenic substrate C_{12}FDG (5-dodecanoylaminofluorescein-di- β -galactopyranoside). Culture medium was substituted for 100 nmol/l Bafilomycin A1 (Tocris R&D Systems) in serumfree DMEM for lysosomal alkalization and incubated for 1 h at 37°C . Subsequently, 50 $\mu\text{mol/l}$ $\text{C}_{12}\text{FDG-FITC}$ (Life Technologies) in serum-free DMEM was added. After 1 h incubation (37°C) the percentage of senescent cells (high FITC and high SSC signal) was measured by LSRII cytometer (BD Biosciences) and analyzed with FACSDiva Software (BD Biosciences).

Western blot analysis

Cells were lysed (Cell Signaling), sonicated and centrifuged (13.000 x g, 10 min, 4°C). Protein concentration was determined by BCA Protein Assay Kit (Pierce). Extracts were supplemented with Roti@Load 1 loading buffer (Roth), boiled (10 min, 95°C) and stored (-20°C). After SDS-PAGE (stacking gel: 2.7 ml ddH_2O , 0.67 ml acrylamide, 0.5 ml Tris-HCl (pH 6.8), 40 μl SDS (10%), 40 μl APS (10%), 4 μl TEMED; separating gel: 5.7 ml ddH_2O , 1.7 ml acrylamide, 2.5 ml Tris-HCl (pH 6.8), 100 μl SDS (10%), 100 μl APS (10%), 16 μl TEMED), proteins were transferred to a PVDF (polyvinylidene fluoride) membrane. After blocking (5% milk), PVDF

membranes were incubated with primary antibodies (12 h, 4°C) anti-BRCA2 (Calbiochem, #OP95), anti-ORC2 (BD Pharmingen, #559266), anti-HSP 70 (Cell signaling, #4876 and #4876), anti-HSP 90 (Cell signaling #4875) or anti- β -actin (Cell signaling #4967) and subsequently (1 h, room temperature) with secondary antibodies (Cell signaling, anti-mouse #7076, anti-rabbit #7074 or anti-rat #7077). Visualization was performed by ECL Western Blot detection reagent (GE Healthcare) on X-ray films and semiquantitative densitometric analysis by ImageJ.

Immunostaining and confocal microscopy

Cells were seeded on glass coverslips. 4 hrs after treatment, cells were fixed (2% PFA), permeabilized (0.5% Triton X-100) and blocked (2% BSA). Subsequently, incubation with primary antibodies mouse anti-phospho-Histone H2AX (Ser139) (Millipore, # 05-636) and rabbit anti-RAD51 (Calbiochem, # PC130) (1 h, room temperature), staining with the relevant secondary antibodies Alexa Fluor 546 goat anti-mouse IgG (Invitrogen, # A-11030) and Alexa Fluor 488 goat anti-rabbit IgG (Invitrogen, # A-11008) (1 h, room temperature), counterstaining with DAPI and mounting with Vectashield (Vector Laboratories) was performed. Images were obtained using Leica TCS SP5 II confocal microscope Leica image analysis software (LAS AF).

Cell transfection with siRNAs

At a confluency of 50-60%, cells were transfected with 7.5 nmol/l of siRNA of the BRCA2 GeneSolution siRNA (Qiagen) using 12 μ l HiPerFect transfection reagent (Qiagen) per siRNA in 100 μ l OptiMEM® according to the manufacturer's instructions. Clonogenic assays or immunoblotting were performed 48 hrs and 72 hrs after transfection.

Patients and samples

Treatment with trabectedin and regional hyperthermia: Consenting patients with locally advanced, chemotherapy-refractory high-grade liposarcoma treated between July 2011 and May 2012 according the Institutional Sarcoma Board at the University of Munich were included. Trabectedin (1.5 mg/m²) was given as a 24 hrs i.v.-infusion every 3 weeks according to European guidelines (26). After toxicities, dose was reduced according to the manufacturer's recommended algorithm (1.5 or 1.0 mg/m²).

At the end of infusion, regional hyperthermia was applied for 90 min (temperature range 40°C – 43°C) in accordance to the European Society for Hyperthermic Oncology (ESHO) guidelines (27). Retrospective analysis was approved by the Ethical Committee of the University of Munich (UE-NR123-13). The interval between date of first cycle trabectedin and progression according to RECIST criteria (28) or last follow up (progression free survival, PFS) respectively death or last follow up (overall survival, OS) was evaluated. Toxicities (hematological, renal and hepatic) were graded according to the CTCAE (Version 4.0) of the National Cancer Institute (NCI).

Phosphorylation of H2AX in PBMCs: Blood samples were taken at 0, 20, and 24 hrs after start of trabectedin infusion for immunostaining of γ H2AX in order to detect DSB foci in peripheral blood mononuclear cells (PBMCs). For preparation, 10 ml of whole blood collected in heparinized sampling tubes were diluted with 10 ml HBSS. 8 ml of the mixture were loaded on 3 ml Ficoll separation solution (Sigma) and centrifuged (1500 g, 30 min, room temperature). The white cell interface was collected, resuspended in 10 ml HBSS and centrifuged again (350 g, 10 min). Finally, PBMCs were washed in PBS and stored at -20°C. Cells were fixed (2% PFA) and permeabilized (90% methanol). Subsequently, PBMCs were transferred to slides using a cytopsin and blocked with 1% BSA for 1 h. The cells were probed with anti-phospho-H2AX (Ser139) antibody (Millipore) overnight at 4°C followed by a 1 h incubation at room temperature with the secondary antibody (Cy-3 goat anti-mouse IgG (Jackson ImmunoResearchLab). Nuclear counterstaining was performed with Hoechst 33342 (Sigma) and cover slips were mounted with Vectashield (Vector Laboratories). Images were obtained using an LSM510 and processed using LSM5 image analysis software (Zeiss).

Statistical analyses

In vitro results are expressed as values, means + SEM of at least 3 independent experiments. Where indicated, data were analyzed using univariate ANOVA and p-values < 0.05 or < 0.01 are indicated with “*” or “**”. Survival (PFS, OS) was analyzed according to the Kaplan-Meier method. All statistical calculations were performed using SPSS (SPSS Statistics Version 22) software. For patient samples, ANOVA with repeated measurements was used to assess the additional effect of heat to an assumed monotonic trabectedin kinetic.

Results

Chemosensitization to trabectedin by hyperthermia

We first performed time course experiments analyzing the clonogenic survival of human sarcoma cell lines. In particular, an optimized treatment schedule achieving best effectiveness *in vitro* while resembling most suitably the conditions of the clinical setting had to be established. Therefore, we tested three treatment sequences: Hyperthermia for 90 min at 41.8°C or 43°C applied directly before, directly after or concurrently during trabectedin exposure for 180 min.

U2OS showed only a minor reduction of clonogenic survival after trabectedin (1-2 nmol/l) treatment at 37°C but the effect was remarkably enhanced by hyperthermia at 41.8°C and at 43°C (Fig. 1A-C, left column). After correction for hyperthermia, the enhancement of trabectedin effectiveness is clearly evident for all three regimens by the significant divergence of the curves at 41.8°C or 43°C compared to 37°C showing obviously strong chemosensitization to trabectedin by heat (Fig. A-C, right column). Only for the trabectedin-before-hyperthermia-sequence, the corrected graphs of 37°C and 41.8°C are not diverging but on the top of each other suggesting at least an additive effect.

The application at the end of concurrent exposure to trabectedin (Fig. 1D) showed the strongest effect of chemosensitization (Fig. 1C). Next, we evaluated our results in cell lines of further sarcoma entities. The cell lines SW872 (liposarcoma) and SW982 (synovial sarcoma) were subjected to the concurrent exposure regimen of trabectedin (1-4 nmol/l) and hyperthermia (41.8°C or 43°C) as drafted in Fig. 1D. All cells tested displayed a dose-dependent decrease in clonogenic survival. In SW982, slightly higher trabectedin susceptibility was seen. In SW872 and SW982, we again detected a strong enhancement of trabectedin effectiveness in addition to the heat effect (Fig. 2, left column). Like in U2OS, the occurring thermal enhancement of trabectedin is clearly evident by the significant divergence of the curves at 41.8°C or 43°C compared to 37°C after correction for hyperthermia (Fig. 2, right column). As control, we tested the hyperthermia response by Western blot analysis of the HSP 90 protein and the inducible HSP70 protein in several sarcoma cell lines (U2OS, SW872 and SKUT-1). As expected, both temperatures did not influence HSP90 expression but enhanced HSP70 expression independently of trabectedin treatment (Fig. S2).

Cell cycle arrest and induction of apoptosis or senescence

In order to investigate the underlying cellular mechanisms of heat-mediated chemosensitization, we analyzed the cell cycle kinetics after concurrent treatment with trabectedin (5-20 nmol/l) and hyperthermia (41.8°C, 43°C). Fig. 3A shows DNA content-histograms of SW872 (left) and U2OS (right) 24 and 48 hrs after treatment (10 nmol/l trabectedin). In both cell lines, trabectedin caused a marked G2/M-arrest after 24 hrs, which was strongly enhanced by additional hyperthermia (upper row). 48 hrs after treatment, cells treated with trabectedin at 37°C started to recover and the DNA histograms started to return to an almost normal shape. In contrast, treatment with additional hyperthermia prolonged trabectedin induced cell cycle arrest in both investigated cell lines (lower row). Hyperthermia alone caused no significant alterations in cell cycle distributions (data not shown).

To investigate the cell fate of heat enhanced G2/M-arrested cells, we analyzed apoptosis and caspase-activation in SW872 and U2OS after concurrent treatment with trabectedin and hyperthermia. In SW872, a dose-dependent increase in the number of apoptotic cells within the sub G1 population paralleled by strong activation of caspase-3 and -7 was observed (Fig. 3B and 3C, upper row). In contrast, U2OS barely underwent apoptosis and only marginal caspase activation was detected (Fig. 3B and Fig. 3C, lower row).

Additionally, we assessed induction of senescence in response to the treatments. Particularly U2OS – instead of undergoing apoptosis – showed a strong senescence response and a heat-dependent continuously increasing number of senescent cells over 72 hrs (data not shown) to 144 hrs (Fig. 3D, lower row). In comparison, SW872, which preferentially underwent apoptosis, showed no detectable induction of senescence (Fig. 3D, upper row). In summary, hyperthermia enhances trabectedin-induced G2/M-arrest followed by a cell line dependent induction of apoptosis or senescence.

Degradation of BRCA2 by hyperthermia

Based upon the previous report of heat-inducible degradation of BRCA2 (21), we examined BRCA2 protein levels upon concurrent treatment with trabectedin and hyperthermia. Immunoblotting in several human sarcoma cell lines (SW982, SW872, U2OS) and in one colorectal cancer cell line (DLD1) revealed that BRCA2 is decreased strongly after hyperthermia (41.8°C and 43°C) in a temperature-

dependent manner. Incubation with trabectedin did not influence BRCA2 expression (Fig. 4A and 4B).

Increase of H2AX phosphorylation and impaired RAD51 colocalization

Because of the known trabectedin related induction of DSBs, we analyzed the appearance of DSB-positive cells (≥ 5 H2AX foci per nucleus) after concurrent treatment with trabectedin and hyperthermia by immunostaining of phosphorylated H2AX (γ H2AX) which is a key marker for DSBs. In Fig. 4C, confocal images and the percentage of DSB-positive cells with or without trabectedin and/or hyperthermia (41.8°C and 43°C) are shown. The proportion of DNA-damaged cells was remarkably increased after additional hyperthermia at both temperatures compared to the effect of trabectedin or hyperthermia alone, respectively. These results led us to hypothesize that heat-mediated BRCA2 degradation and impairment of HRR might be involved in the accumulation of DSBs. Hence, we examined the colocalization of RAD51 with γ H2AX, since this implies an intact HRR cascade. Confocal microscopy revealed that the recruitment of RAD51 to γ H2AX foci was attenuated after concurrent hyperthermia at 41.8°C and almost completely abolished after 43°C (Fig. 4D). The densitometric analysis (Fig. 4D) clearly demonstrates that – when treated without hyperthermia – the majority of DSB-positive cells ($\geq 90\%$) display a colocalization of γ H2AX and RAD51 which suggests an intact HRR. After concurrent hyperthermia, the percentage of colocalization decreases significantly to $< 70\%$ at 41.8°C and $< 40\%$ at 43°C, respectively.

Chemosensitization to trabectedin is restricted to BRCA2-proficient cells

The role of heat-mediated BRCA2 degradation in trabectedin chemosensitization was further investigated in BRCA2-deficient cells using a human colon carcinoma cell line (DLD1) lacking BRCA2 (DLD1 *BRCA2*^{-/-}) and U2OS transfected with BRCA2-targeting siRNAs (U2OS BRCA2-KD). In Fig. 5A, the clonogenic survival curves after concurrent treatment and corrected for the toxicity of hyperthermia are shown for DLD1 *BRCA2*^{-/-} and U2OS BRCA2-KD cells (Fig. 5A, right column) and the respective control cells DLD1 parental and mock-treated U2OS (Fig. 5A, left column). The additional gain in trabectedin effectiveness after concurrent hyperthermia is clearly evident in both BRCA2-proficient control cells by the significant divergence of the curves at 41.8°C or 43°C compared to 37°C and abolished in the BRCA2-

deficient/-silenced cells. However, the effectiveness of trabectedin in mock-transfected U2OS was lower than in untransfected cells, which can be explained by reduced ERCC5 expression after transfection (Fig S3). Comparing the cell cycle distributions of treated DLD1 parental and DLD1 *BRCA2*^{-/-} cells, heat-associated amplification of G2/M phase arrest was only detectable in the *BRCA2*-proficient cell line (Fig. 5B). Moreover, the reinforced induction of apoptosis by the combined treatment was clearly diminished in DLD1 *BRCA2*^{-/-} cells compared to DLD1 parental cells (Fig 5C). As expected, DLD1 *BRCA2*^{-/-} cells displayed an increased induction of apoptosis by trabectedin alone in comparison to *BRCA2*-proficient control cells (Fig. 5C).

Trabectedin and regional hyperthermia in patients

Four patients with anthracycline-refractory, progressive high-risk soft-tissue sarcoma (liposarcomas) were treated with trabectedin and regional hyperthermia. The treatment schedule is depicted in Fig. 6A. The patients received a mean of 4 cycles (range: 2-6) of trabectedin (1.5 mg/m²) as 24 hrs i.v.-infusion combined with regional hyperthermia, repeated every 3 weeks. In terms of treatment related toxicity, 9 events of grade 3/4 toxicities (6 hematological, 3 hepatic) occurred. Toxicities were well managed with dose adjustments of trabectedin (from 1.25 to 1.0 mg/m²). Progression arrest was seen in three patients and median progression free survival was 4.1 months (range 1.0 to 20.4 months). With a median follow-up of 16.7 months (range: 4.6 to 28.9 months), observed median survival was +12.9 months (range: 4.5 to 29 months).

γ H2AX foci in PBMCs as potential surrogate marker for heat-enhanced trabectedin effectiveness

Repeated analysis of DSBs in PBMCs by immunostaining and microscopy showed a 2.5-fold increase in DSB-positive cells (≥ 5 γ H2AX foci per nucleus) compared to baseline level after 20 hrs and a 4.9-fold increase after 24 hrs of trabectedin combined with regional hyperthermia (Fig. 6B and 6C). The exploratory statistical analysis showed a highly significant regional hyperthermia effect to an assumed monotonic trabectedin kinetic on the potential surrogate marker DSB ($p < 0.01$).

Discussion

Our results demonstrate an increase of trabectedin effectiveness by additional hyperthermia in several sarcoma models. Hyperthermia was applied at two temperatures (41.8°C and 43°C) mimicking the heterogeneous temperature profile achieved clinically in sarcomas by regional hyperthermia with spatial temperature gradients within the heated tumor (29). For clinical application of trabectedin combined with hyperthermia, the preclinical identification of an optimal sequence is important. Therefore, we tested three different treatment schedules. Addition of hyperthermia at the end of concurrent exposure to trabectedin was the most effective sequence. At present and influenced by this observation, we use this schedule in the context of a 24 hrs i.v.-infusion of trabectedin in patients treated in our institution.

The observed thermal enhancement of effectiveness was achieved *in vitro* after short exposure to trabectedin at pharmacological relevant concentrations (nmol/l) which approximate to the peak plasma-concentrations of approximately 2 nmol/l observed in patients (30). With regard to trabectedin susceptibility, the IC₅₀ concentrations we found in SW872, SW982 and SKUT-1 after incubation for 72 hrs (data not shown) were consistent with previously reported IC₅₀ concentrations of trabectedin in a wide range of sarcoma and carcinoma cell lines (31).

In all investigated cell lines, combined treatment clearly enhanced antitumor effectiveness of trabectedin. By correction for heat cytotoxicity, the more than additive growth inhibition was obvious in three (U2OS, SW872, and SW982) of five sarcoma cell lines as well as in an additionally investigated colon-carcinoma cell line (DLD1). However, in two lines (RD-ES and SKUT-1) the enhanced effectiveness of the combination was weaker with no significant divergence of the survival curves after correction for hyperthermia (data not shown). Nevertheless, in all investigated cell lines a cytotoxic effect of hyperthermia alone was obvious. A potential interference of the heat shock response by trabectedin as previously reported to block the transcriptional activation of the HSP70 promoter (32) could be excluded in our study because of the regular induction of the Hsp70 protein after combined treatment.

The observed chemosensitization was independent of trabectedin susceptibility at 37°C (e.g. SW872). This is consistent with observations regarding other anticancer

agents, that heat adds to chemotherapy by the thermal enhancement of drug efficacy even at non-toxic concentrations and the direct heat-related cytotoxicity (13). Furthermore, we demonstrate major effects of combined treatment on the cell cycle in terms of G2/M-arrest as shown for U2OS and SW872. The observed enhanced drug effectiveness parallels the impairment of HRR in late S-phase (16). Accordingly, it was shown that cells in the S-phase are most vulnerable with regard to heat (33). An arrest of cells in the G2/M phase induced by trabectedin alone was discussed with regard to different degrees of radiosensitization (34,35). Radiosensitivity of cells changes within progression of the cell cycle. While cells in the S-phase are particularly radioresistant, cells in the G2/M phase are considered as the most radiosensitive. Therefore, additional radiation after induction of G2/M-arrest by trabectedin and heat might be an interesting treatment option to be tested in the future.

Although combined treatment generally reduced clonogenic survival and enhanced G2/M-arrest, we found specific differences in cellular treatment responses. Trabectedin dose-dependently induced apoptosis in SW872 and senescence in U2OS, which both was significantly amplified by additional hyperthermia. In general, the p53 activity (for known TP53 mutations in used cell lines see Fig S1) is crucial for the activation of senescence or apoptosis programs in response to cellular stress or DNA damage (36). In some cells, p53 might preferentially activate senescence (37). Therefore, mutated p53 as well as elevated expression of the p53 negative regulator MDM2 (38) might be causative for observed apoptosis in SW872 and unaffected p53 signaling for senescence in U2OS. Furthermore, it was reported that mutations or deletions of the *TP53* gene in sarcoma cells increases sensitivity to trabectedin (39) whereas regular p53 expression is related to susceptibility to heat alone (40). After heat exposure without trabectedin (41.8°C or 43°C), however, we found no significant induction of apoptosis or senescence in SW872 and U2OS. In contrast, hyperthermia alone was shown to induce apoptosis in U2OS beginning at 43°C with remarkably greater amounts of apoptotic cells after temperatures of 45°C and higher (41). Different heat doses applied or other methodical differences can explain why we detected nearly no induction of apoptosis at 43°C. To the best of our knowledge, there is currently no suitable report showing direct induction of senescence by heat alone. Given the tumor suppressive potential of senescence, discovering novel

senescence-inducing interventions for the treatment of cancer including sarcomas is of great interest (42). Whether trabectedin with additional hyperthermia offers such intervention in p53 proficient tumor-cells – as seen in U2OS – has to be addressed further.

We found that the BRCA2 protein level is significantly and temperature-dose-dependently decreased in all investigated cell lines: U2OS, SW872, SW982 and DLD1 as well as in RD-ES and SKUT-1. BRCA2 expression level was not influenced by trabectedin alone. In SKUT-1 and especially in RD-ES, the heat-dependent degradation of BRCA2 was less pronounced (data not shown). Accordingly, in these two cell lines the effectiveness of combined treatment was weaker with no significant divergence of the survival curves after correction for hyperthermia. This suggests that the strength of thermal enhancement of trabectedin is correlated to induced BRCA2 deficiency. Nevertheless, the observed consistent BRCA2 degradation by heat implies that this is a general effect of hyperthermia, which also might be utilized in a wider range of tumor entities.

Furthermore, the amount of DSB-positive cells (≥ 5 γ H2AX foci per nucleus) rose significantly after combined treatment. We speculate that the heat-induced increase might be explained by the inability of BRCA2-deficient cells to repair DSBs due to missing recruitment of RAD51 to the DNA damage sites. Consistent with the defined role of BRCA2 in the control of RAD51 mediated recombination (43), our data support this mechanism by the highly significant temperature dependent decline of colocalizations of γ H2AX and RAD51 after combined treatment without decrease in RAD51 protein levels after hyperthermia (21). Consequently, the DNA-damage within one cell starts to accumulate without being repaired properly, which is responsible for observed G2/M block and induction of apoptosis or senescence. Further prove of evidence that the observed effects of the combined treatment are linked to heat-mediated BRCA2 degradation derives from our results using the BRCA2 knockout cell line (DLD1 *BRCA2*^{-/-}) and the siRNA knockdown of BRCA2 in U2OS. The lack of thermal enhancement in BRCA2-silenced cells supports that HRR deficiency is the key for heat modulation of trabectedin effectiveness. In our study, we demonstrate the role of BRCA2 as the major responsible heat target. However, more challenging molecular experiments beyond the scope of our investigations are needed to exclude

other potentially heat-sensitive candidates which might be also involved in the mechanisms (44). Xian et al. (2003) reported that BRCA1, a further HRR protein, is also degraded after hyperthermia (17). In another study, BRCA1 depletion in U2OS cells resulted only in a modest reduction of BRCA2 and RAD51 positive repair foci, but occurrence of repair foci was strongly dependent upon PALB2 expression. Therefore, the authors suggest that BRCA1 is involved in modulation and stabilization of the PALB2 dependent loading of BRCA2 and RAD51 at the DSBs (45). Altogether, heat-mediated degradation of BRCA1 might additionally enhance chemosensitization of trabectedin but to our opinion cannot explain observed strong reduction in RAD51 colocalizations, which is very likely linked to BRCA2 degradation. In Fig. 6.D an adapted scheme (45) showing proteins involved in hyperthermia mediated HRR inhibition is depicted.

To our knowledge, this is the first report showing the enhanced cytotoxicity of trabectedin by hyperthermia-induced impairment of HRR. In addition to recently reported activity of trabectedin in pretreated breast cancer patients restricted to germline or somatic BRCA1/2 mutations (46), the on-demand induction of BRCA-ness might open a new window for the more extended use of trabectedin in BRCA2-proficient tumors if heat treatment is added. Furthermore, there is strong evidence that targeting BRCA2 in tumors with intact HRR may enhance effectiveness of several anti-tumor treatments. For example, interrupted DNA repair may contribute to a significant augmentation of DNA damage, which induces anti-tumor programs like apoptosis or senescence. Moreover, generation of further genetic heterogeneity or acquirement of treatment resistance is expected to be reduced by the inhibition of DNA damage repair. Accordingly, Rytelewski et al. (2014) showed that the antisense oligodeoxynucleotide transfection of BRCA2 sensitizes cell lines of several tumor entities to cisplatin. There is also clinical evidence for a beneficial role of BRCA2 mutations in cancer patients. For example, patients with BRCA2 mutated ovarian cancer had improved outcome after primary therapy (48) and in patients with BRCA2 mutated breast cancer the tendency towards a lower risk of tumor recurrence or occurrence of metastases was described (49).

Our retrospective analysis of patients shows feasibility of the combined treatment schedule without uncommon side effects. The observed clinical outcome with a

progression arrest in three out of four patients and with median survival of +12.9 months is promising compared to other clinical studies investigating trabectedin (1). We investigated γ H2AX in blood cells of patients treated with regional hyperthermia and trabectedin in a similar approach as successfully used in the context of local radiotherapy as surrogate marker for induced DSBs (50). PBMCs taken from these patients revealed an increase in γ H2AX foci most likely due to the addition of heat. Because of the off-target activity of trabectedin in blood monocytes and macrophages (8) and effects on the microenvironment of tumors (9) this observation might be the first step in defining surrogate markers for clinical efficacy.

In conclusion, these data support the use of trabectedin combined with hyperthermia to treat sarcoma. The mechanisms of action seem to be related to BRCA2 degradation by heat. However, further clinical and preclinical studies are needed to explore whether the demonstrated thermal enhanced effectiveness of trabectedin can be translated to beneficial outcomes of patients. In soft-tissue sarcomas, a phase II randomized clinical trial (Hyper-TET – **hyper**thermia **enhanced** trabectedin, clinicaltrials.gov: NCT02359474) is underway to test this hypothesis (primary endpoint: PFS; secondary endpoints: Treatment response, OS and toxicities).

Acknowledgements

This study was supported by Helmholtz Association (VH -VI -140). We are indebted to the patients who took part in the retrospective analysis. For proofreading we thank Adnan Tanović, PharmaMar, Spain.

References

1. Samuels BL, Chawla S, Patel S et al. Clinical outcomes and safety with trabectedin therapy in patients with advanced soft tissue sarcomas following failure of prior chemotherapy: Results of a worldwide expanded access program study. *Ann Oncol* 2013;24:1703–9.
2. D'Incalci M, Galmarini CM. A review of trabectedin (ET-743): a unique mechanism of action. *Mol Cancer Ther* 2010;9:2157–63.
3. Herrero AB, Martín-Castellanos C, Marco E, et al. Cross-talk between nucleotide excision and homologous recombination DNA repair pathways in the mechanism of action of antitumor trabectedin. *Cancer Res* 2006;66:8155–62.
4. Laroche-Clary A, Chaire V, Le Morvan V et al. BRCA1 haplotype and clinical benefit of trabectedin in soft-tissue sarcoma patients. *Br J Cancer* 2015;112:688–92.
5. Schöffski P, Taron M, Jimeno J et al. Predictive impact of DNA repair functionality on clinical outcome of advanced sarcoma patients treated with trabectedin: A retrospective multicentric study. *Eur J Cancer* 2011;47:1006–12.
6. Italiano A, Laurand A, Laroche A et al. ERCC5/XPG, ERCC1, and BRCA1 gene status and clinical benefit of trabectedin in patients with soft tissue sarcoma. *Cancer* 2011;117:3445–56.
7. Allavena P, Signorelli M, Chieppa M et al. Anti-inflammatory properties of the novel antitumor agent Yondelis (Trabectedin): Inhibition of macrophage differentiation and cytokine production. *Cancer Res* 2005;65:2964–71.
8. Germano G, Frapolli R, Belgiovine C et al. Role of Macrophage Targeting in the Antitumor Activity of Trabectedin. *Cancer Cell* 2013;23:249–62.
9. Germano G, Frapolli R, Simone M et al. Antitumor and anti-inflammatory effects of trabectedin on human myxoid liposarcoma cells. *Cancer Res* 2010;70:2235–44.
10. Wust P, Hildebrandt B, Sreenivasa G, et al. Hyperthermia in combined treatment of cancer. *Lancet Oncol* 2002;3:487–97.
11. Issels RD, Lindner LH, Verweij J et al. Neo-adjuvant chemotherapy alone or with regional hyperthermia for localised high-risk soft-tissue sarcoma: A randomised phase 3 multicentre study. *Lancet Oncol* 2010;11:561–70.
12. Hildebrandt B, Wust P, Ahlers O, et al. The cellular and molecular basis of hyperthermia. *Crit Rev Oncol Hematol* 2002;43:33-56
13. Issels RD. Hyperthermia adds to chemotherapy. *Eur J Cancer* 2008;44:2546–54.
14. Dahm-Daphi J, Brammer I, Dikomey E. Heat effects on the repair of DNA double-strand breaks in CHO cells. *Int J Radiat Biol* 1997;72:171–9.
15. Kampinga HH, Jorritsma JB, Konings AWT. Heat-induced alterations in DNA polymerase activity of HeLa cells and of isolated nuclei. Relation to cell survival. *Int J Radiat Biol Relat Stud Phys Chem Med* 1985;47:29–40.
16. Genet SC, Fujii Y, Maeda J et al. Hyperthermia inhibits homologous recombination repair and sensitizes cells to ionizing radiation in a time- and

- temperature-dependent manner. *J Cell Physiol* 2013;228:1473–81.
17. Xian Ma Y, Fan S, Xiong J et al. Role of BRCA1 in heat shock response. *Oncogene* 2003;22:10–27.
 18. Rogakou EP, Pilch DR, Orr AH et al. DNA double-stranded breaks induce histone H2AX phosphorylation on serine 139. *J Biol Chem* 1998;273:5858–68.
 19. Burma S, Chen BP, Murphy M et al. ATM phosphorylates histone H2AX in response to DNA double-strand breaks. *J Biol Chem* 2001;276:42462–7.
 20. Redon CE, Weyemi U, Parekh PR et al. γ -H2AX and other histone post-translational modifications in the clinic. *Biochim Biophys Acta - Gene Regul Mech* 2012;1819:743–56.
 21. Krawczyk PM, Eppink B, Essers J et al. Mild hyperthermia inhibits homologous recombination, induces BRCA2 degradation, and sensitizes cancer cells to poly (ADP-ribose) polymerase-1 inhibition. *Proc Natl Acad Sci U S A* 2011;108:9851–6.
 22. Davies AA, Masson J-Y, McIlwraith MJ et al. Role of BRCA2 in control of the RAD51 recombination and DNA repair protein. *Mol Cell* 2001;7:273–82.
 23. Patel KJ, Yu VP, Lee H et al. Involvement of Brca2 in DNA repair. *Mol Cell* 1998;1:347–57.
 24. Franken NAP, Rodermond HM, Stap J et al. Clonogenic assay of cells in vitro. *Nat Protoc* 2006;1:2315–9.
 25. Gary RK, Kindell SM. Quantitative assay of senescence-associated -galactosidase activity in mammalian cell extracts. *Anal Biochem* 2005;343:329–34.
 26. The ESMO/European Sarcoma Network Working Group. Soft tissue and visceral sarcomas: ESMO Clinical Practice Guidelines for diagnosis, treatment and follow-up. *Ann Oncol* 2014;25 Suppl 3:iii113–23.
 27. Bruggmoser G, Bauchowitz S, Canters R et al. Quality assurance for clinical studies in regional deep hyperthermia. *Strahlentherapie und Onkol* 2011;187:605–10.
 28. Eisenhauer EA, Therasse P, Bogaerts J et al. New response evaluation criteria in solid tumours: Revised RECIST guideline (version 1.1). *Eur J Cancer* 2009;45:228–47.
 29. Issels RD, Prenninger SW, Nagele A et al. Ifosfamide plus etoposide combined with regional hyperthermia in patients with locally advanced sarcomas: A phase II study. *J Clin Oncol* 1990;8:1818–29.
 30. Kesteren C Van, Cvitkovic E, Taamma A et al. Pharmacokinetics and pharmacodynamics of the novel marine-derived anticancer agent ecteinascidin 743 in a phase I dose-finding study. *Clin Cancer Res* 2000;6:4725–32.
 31. Li WW, Takahashi N, Jhanwar S et al. Sensitivity of soft tissue sarcoma cell lines to chemotherapeutic agents: Identification of ecteinascidin-743 as a potent cytotoxic agent. *Clin Cancer Res* 2001;7:2908–11.
 32. Minuzzo M, Marchini S, Brogginini M et al. Interference of transcriptional activation by the antineoplastic drug ecteinascidin-743. *Proc Natl Acad Sci U S A* 2000;97:6780–4.
 33. Lauber K, Brix N, Ernst A et al. Targeting the heat shock response in

- combination with radiotherapy: Sensitizing cancer cells to irradiation-induced cell death and heating up their immunogenicity. *Cancer Lett* 2015;368:209-29.
34. Simoens C, Korst AEC, De Pooter CMJ et al. In vitro interaction between eteinasclidin 743 (ET-743) and radiation, in relation to its cell cycle effects. *Br J Cancer* 2003;89:2305-11.
 35. Romero J, Zapata I, Córdoba S et al. In vitro radiosensitisation by trabectedin in human cancer cell lines. *Eur J Cancer* 2008;44:1726-33.
 36. Rufini A, Tucci P, Celardo I, Melino G. Senescence and aging: the critical roles of p53. *Oncogene* 2013;32:5129-43.
 37. Campisi J, d'Adda di Fagagna F. Cellular senescence: when bad things happen to good cells. *Nat Rev Mol Cell Biol* 2007;8:729-40.
 38. Ohnstad HO, Castro R, Sun J et al. Correlation of TP53 and MDM2 genotypes with response to therapy in sarcoma. *Cancer* 2013;119:1013-22.
 39. Moneo V, Serelde BG, Fominaya J et al. Extreme sensitivity to Yondelis® (Trabectedin, ET-743) in low passaged sarcoma cell lines correlates with mutated p53. *J Cell Biochem* 2007;100:339-48.
 40. Ohnishi K, Takahashi A, Yokota S et al. Effects of a heat shock protein inhibitor KNK437 on heat sensitivity and heat tolerance in human squamous cell carcinoma cell lines differing in p53 status. *Int J Radiat Biol* 2004;80:607-14.
 41. Hou C-H, Lin F-L, Hou S-M et al. Hyperthermia Induces Apoptosis through Endoplasmic Reticulum and Reactive Oxygen Species in Human Osteosarcoma Cells. *Int J Mol Sci* 2014;15:17380-95.
 42. Ventura A, Kirsch DG, McLaughlin ME et al. Restoration of p53 function leads to tumour regression in vivo. *Nature* 2007;445:661-5.
 43. Jensen RB, Carreira A, Kowalczykowski SC. Purified human BRCA2 stimulates RAD51-mediated recombination. *Nature* 2010;467:678-83.
 44. Powell SN, Kachnic LA. Homologous recombination research is heating up and ready for therapy. *Proc Natl Acad Sci U S A* 2011;108:9731-2.
 45. Sy SMH, Huen MSY, Chen J. PALB2 is an integral component of the BRCA complex required for homologous recombination repair. *Proc Natl Acad Sci U S A* 2009;106:7155-60.
 46. Delalogue S, Wolp-Diniz R, Byrski T et al. Activity of trabectedin in germline BRCA1/2-mutated metastatic breast cancer: Results of an international first-in-class phase II study. *Ann Oncol* 2014;25:1152-8.
 47. Rytelowski M, Tong JG, Buensuceso A et al. BRCA2 inhibition enhances cisplatin-mediated alterations in tumor cell proliferation, metabolism, and metastasis. *Mol Oncol* 2014;8:1429-40.
 48. Vencken PMLH, Kriege M, Hoogwerf D et al. Chemosensitivity and outcome of BRCA1- and BRCA2-associated ovarian cancer patients after first-line chemotherapy compared with sporadic ovarian cancer patients. *Ann Oncol* 2011;22:1346-52.
 49. Bayraktar S, Gutierrez-Barrera AM, Lin H et al. Outcome of metastatic breast cancer in selected women with or without deleterious BRCA mutations. *Clin Exp Metastasis* 2013;30:631-42.
 50. Zahnreich S, Ebersberger A, Kaina B et al. Biodosimetry Based on γ -H2AX

Accepted Article

Quantification and Cytogenetics after Partial- and Total-Body Irradiation during Fractionated Radiotherapy. *Radiat Res* 2015;183:432–46.

Figure legends

Fig. 1 Chemosensitization to trabectedin by hyperthermia: Concurrent treatment of trabectedin and hyperthermia induces the strongest effect on clonogenic survival. Diagrams reflect the relative clonogenic survival in dependence on different trabectedin concentration for different hyperthermia conditions. Duration of trabectedin exposure (1 or 2 nmol/l) at 37°C was 180 min. Hyperthermia was scheduled for 90 min at 41.8°C or at 43°C. U2OS were exposed (A) first to hyperthermia and then to trabectedin or (B) to trabectedin followed by hyperthermia, or (C) to hyperthermia during trabectedin treatment. In the latter case, trabectedin was applied for 90 min at 37°C and hyperthermia was applied for 90 min concurrently to further trabectedin exposure. Graphs represent the clonogenic survival (log-scale) at the indicated temperatures without (left) or with correction for the toxicity by hyperthermia alone (right). Values, means + SEM from at least three independent experiments. ANOVA was performed for trabectedin at 2 nmol/l, data are statistically significant for * $p < 0.05$ or ** $p < 0.01$. (D) Schematic illustration for the concurrent application of trabectedin and hyperthermia.

Fig. 2 Chemosensitization to trabectedin by hyperthermia in different human sarcoma cell lines. Diagrams reflect the relative clonogenic survival in dependence on different trabectedin concentration for different hyperthermia conditions. SW872 (A) and SW982 (B) were concurrently treated with trabectedin and hyperthermia. Duration of trabectedin exposure (1-4 nmol/l) was 180 min at 37°C. Hyperthermia (41.8°C or 43°C) was applied for 90 min. Graphs represent relative clonogenic survival (log-scale) at the indicated temperatures without (left) or with correction for the toxicity of hyperthermia (right). Values, means + SEM from at least three independent experiments. ANOVA was performed for trabectedin at 4 nmol/l, data are statistically significant for * $p < 0.05$ or ** $p < 0.01$.

Fig. 3 Combination of trabectedin and hyperthermia results in enhanced and prolonged G2/M-arrest and an increase of apoptosis or senescence. (A) DNA histograms of SW872 and U2OS concurrently treated with trabectedin (10 nmol/l)

and hyperthermia (41.8°C or 43°C). 24 hrs (upper row) or 48 hrs (lower row) after treatment, cells were collected and analyzed by flow cytometry. Histograms are representative for at least three independent experiments. (B) Bar charts showing the percentage of apoptotic cells 72 hrs after concurrent treatment with trabectedin (5- 20 nmol/l) and hyperthermia (41.8°C or 43°C) of SW872 (upper part) and U2OS (lower part). (C) Diagrams showing the activation of caspase-3 and caspase-7 assessed by measurement of DEVDase activity 24, 48 and 72 hrs after concurrent treatment with trabectedin (co.: 0 nmol/l, Tr: 10 nmol/l) and hyperthermia (41.8°C or 43°C) in SW872 (upper part) and U2OS (lower part). (D) Bar charts representing the senescence-associated β -galactosidase activity 144 hrs after concurrent treatment with trabectedin (5-20 nmol/l) and hyperthermia (41.8°C or 43°C) in SW872 (upper part) and U2OS (lower part). Values, means + SEM from at least three independent experiments. In each case, ANOVA was performed for samples treated with equal trabectedin concentrations, data are statistically significant for * $p < 0.05$ or ** $p < 0.01$.

Fig. 4 Hyperthermia leads to degradation of BRCA2 and accumulation of trabectedin-induced DSBs by impaired HRR. (A) BRCA2 (390 kDa) protein expression level was determined in SW982 by Western blot after concurrent treatment with trabectedin (1 or 2 nmol/l) and hyperthermia (41.8°C or 43°C). ORC2 (65 kDa) was the loading control. Western blots are representative for three independent experiments. Similar results were obtained in SW872, U2OS and DLD1 cells. (B) Bar charts representing the densitometric analysis of BRCA2 expression in U2OS, SW872, SW982 and DLD1. (C) Confocal images of U2OS treated with concurrent trabectedin (2 nmol/l) and hyperthermia (41.8°C or 43°C) showing DSB-positive cells by immunostaining of γ H2AX (red) and DNA with DAPI (blue). Below, bar chart representing the number of DSB-positive (≥ 5 γ H2AX foci per nucleus) SW872 (%) after concurrent treatment with trabectedin (0.5 or 2 nmol/l) and hyperthermia (41.8°C or 43°C) is shown. (D) Confocal images of U2OS (upper row) concurrently treated with trabectedin (2 nmol/l) and hyperthermia (41.8°C or 43°C) showing nuclear colocalization of γ H2AX (red) and RAD51 (green) by immunostaining. Below, bar chart representing the number of γ H2AX and RAD51 colocalization positive cells (%) after concurrent treatment with trabectedin (0.5 or 2 nmol/l) and hyperthermia (41.8°C or 43°C) is shown. Scale bars: 10 μ m. Values,

means \pm SEM from at least three independent experiments. In each case, ANOVA was performed for samples treated with equal trabectedin concentrations, data are statistically significant for * $p < 0.05$; ** $p < 0.01$.

Fig. 5 Chemosensitization to trabectedin is abrogated in BRCA2-deficient cells.

(A) Diagrams reflect the relative clonogenic survival in dependence on different trabectedin concentration for different hyperthermia conditions. Clonogenic survival of BRCA2-proficient DLD1 parental and U2OS (left panel) in comparison to BRCA2-deficient DLD1 *BRCA2*^{-/-} and U2OS BRCA2-KD cells (right panel) concurrently treated with trabectedin (1-4 nmol/l) and hyperthermia (41.8°C or 43°C). Graphs represent relative clonogenic survival corrected for the toxicity of hyperthermia. Western blot for BRCA2 expression in U2OS, mock transfected U2OS (neg. control cells) and U2OS BRCA2-KD cells is depicted as insert. (B) Bar charts showing the percentage (%) of G2/M-arrested DLD1 parental and DLD1 *BRCA2*^{-/-} cells after concurrent treatment with trabectedin (5, 10, 20 nmol/l) and hyperthermia (41.8°C and 43°C). Cells were collected 24 hrs after treatment and cell cycle was analyzed by FACS analysis. (C) Bar charts showing the percentage (%) of apoptotic DLD1 parental (left) and DLD1 *BRCA2*^{-/-} (right) cells 72 hrs after concurrent treatment with trabectedin (Tr, 5-20 nmol/l) and hyperthermia (41.8°C or 43°C) as determined by analysis of sub G1 population. Values, means \pm SEM from at least three independent experiments. In (A) ANOVA was performed for the samples treated with the highest trabectedin concentration (4 nmol/l), in (B) and (C) for each samples treated with equal trabectedin concentrations, data are statistically significant for * $p < 0.05$; ** $p < 0.01$.

Fig. 6 Trabectedin combined with Hyperthermia leads to phosphorylation of H2AX in PBMCs.

(A) Treatment schedule of trabectedin (1.5 mg/m²) for 24 hrs i.v.-infusion with regional hyperthermia (RHT) given at the end of concomitant trabectedin infusion. Heparinized blood samples (10 ml) were taken at the time points as indicated before start of trabectedin infusion, during and after regional hyperthermia, and 48 hrs after start of trabectedin infusion (24 hrs recovery time). (B) Confocal images at 0 hrs (before treatment), 20 hrs (during trabectedin infusion), and

24 hrs (immediately after the end of additional regional hyperthermia) showing stainings of nuclear γ H2AX foci in PBMCs separated from patients' blood. (C) Bar chart showing the quantification of the increase of DSB-positive PBMCs at the indicated time intervals. Values, mean \pm SEM for three patients who received trabectedin (Tr) combined with concurrent regional hyperthermia. Assuming monotonic trabectedin kinetics, the exploratory statistical analysis shows a highly significant effect of regional hyperthermia (** $p=0.009$). (D) Adapted scheme (45) showing the relevant pathway of the HRR system and the target proteins of hyperthermia marked by a red border.

Fig. S1 Temperature during hyperthermia. Diagrams reflect the temperature curves during 90 minutes hyperthermia in cell culture experiments and treated tumors in patients. For cell culture experiments, hyperthermia was carried out in incubators (41.8°C or 43°C) and temperature was measured in the culture medium. In patients, increase of temperature in the heated tumor region was measured with thermoprobes. Values, means \pm SEM from at least three independent experiments (incubators) and three different patients.

Fig. S2 Hyperthermia and trabectedin induced expression of Hsp70. Hsp70 (70 kDa) and Hsp90 (90 kDa) protein expression level was determined in SKUT-1 (A) and SW872 (B) by Western blot 2, 6, 12, 18, 24, 48 and 72 hrs after hyperthermia (41.8°C or 43°C, 90 min). β -actin (42 kDa) was the loading control. Western blots are representative for three independent experiments. (C) Bar chart representing the densitometric analysis of Hsp70 expression in U2OS determined by Western blot 8 and 24 hrs after hyperthermia (41.8°C and 43°C). (D) Hsp70 protein expression level was determined in U2OS by Western blot 0, 0.5, 2, 5, 8 and 24 hrs after hyperthermia (41.8°C or 43°C, 90 min) and/or trabectedin (4 nmol/l). β -actin was the loading control. Western blots are representative for three independent experiments. Values, means \pm SEM from at least three independent experiments.

Fig. S3 Transfection with siRNAs targeting BRCA2 affects ERCC5 protein level.

Bar chart representing the densitometric analysis of ERCC5 expression in U2OS determined by Western blot 48 hrs after transfection. Values, means +/- SEM from at least three independent experiments.

Tab. S1 TP53 mutations in used cell lines

Accepted Article

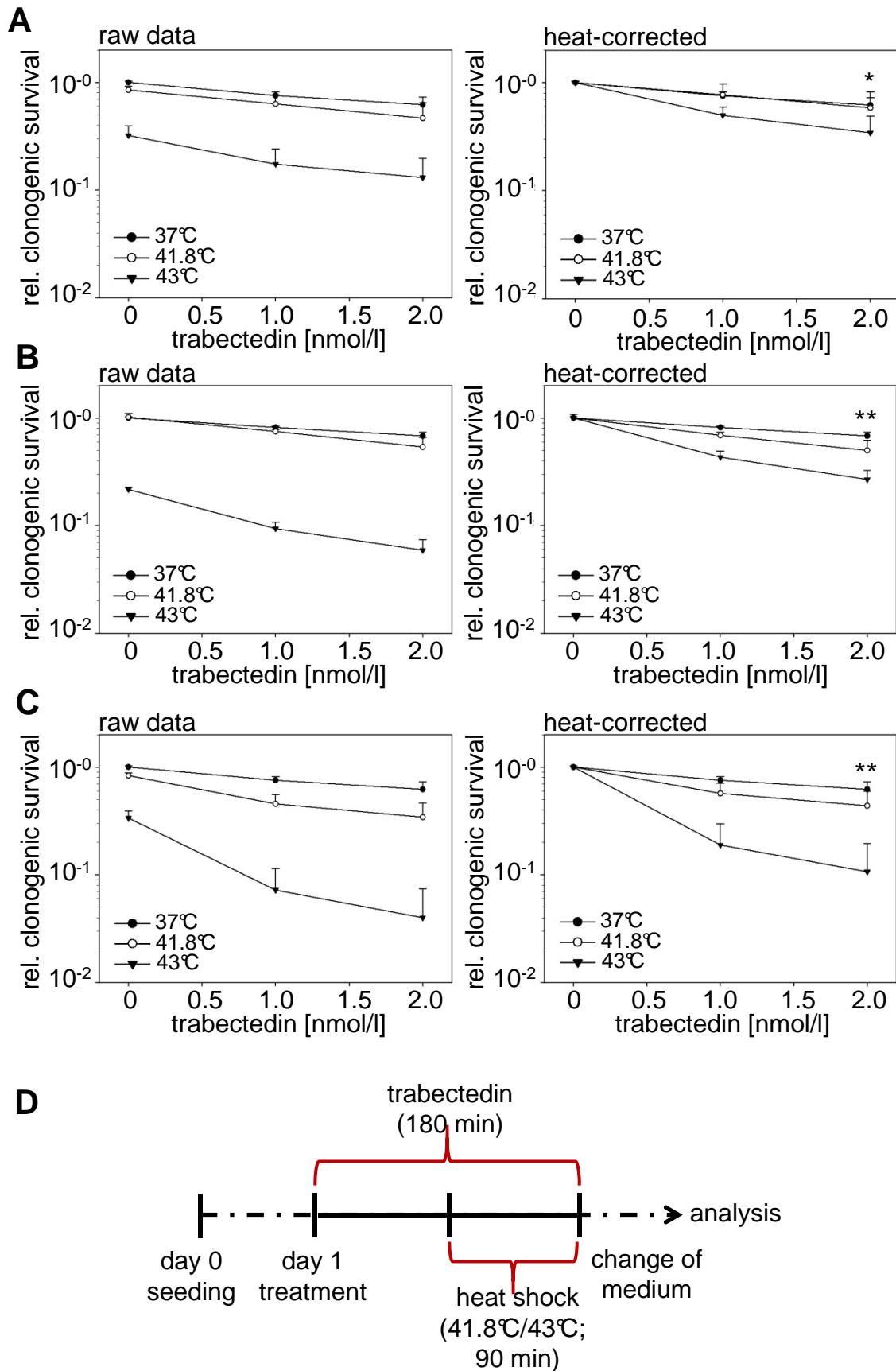
Fig. 1

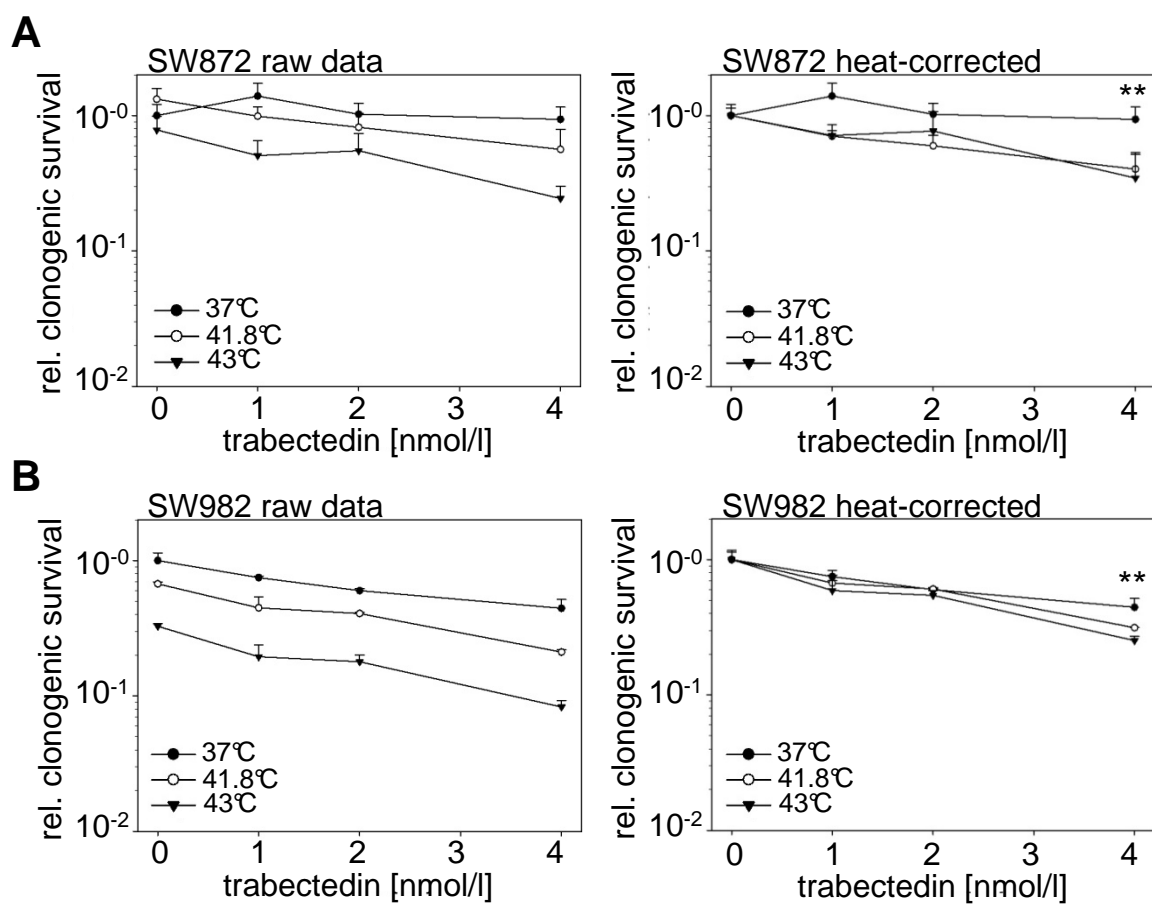
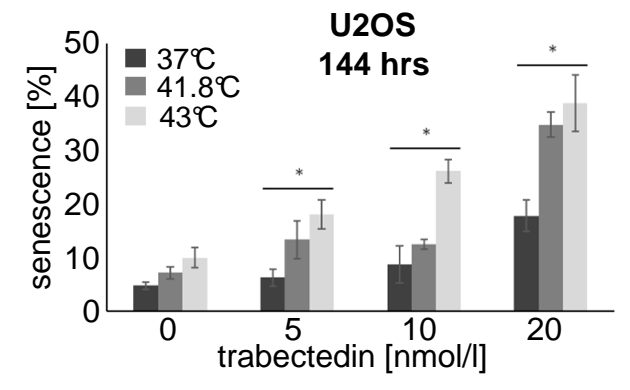
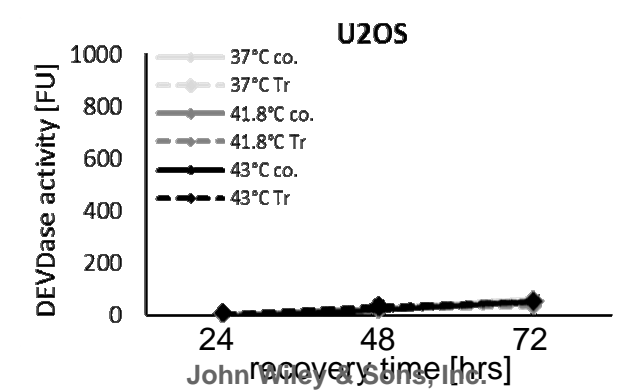
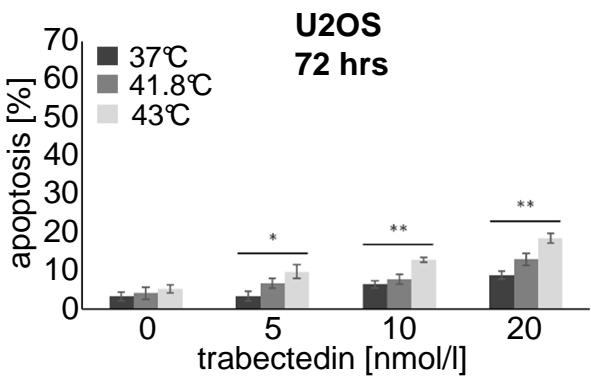
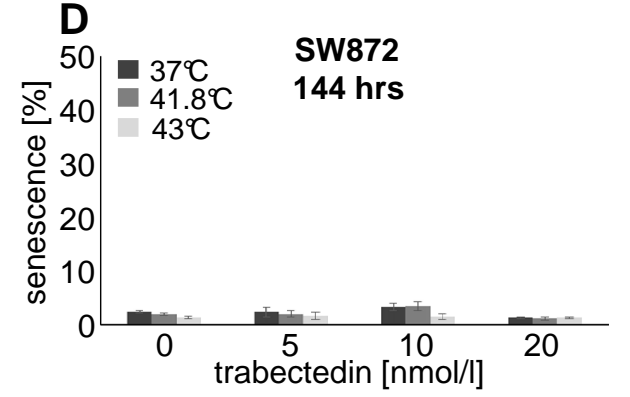
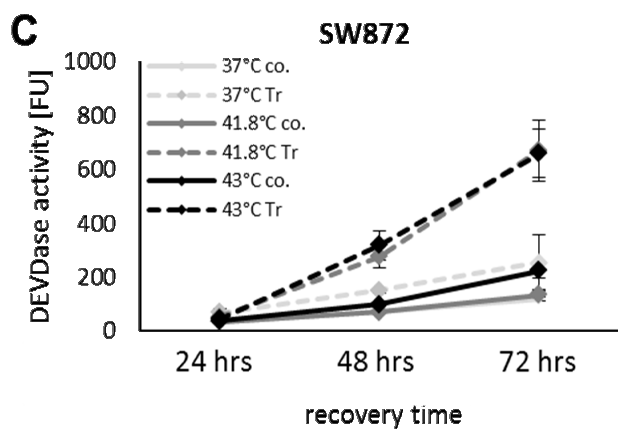
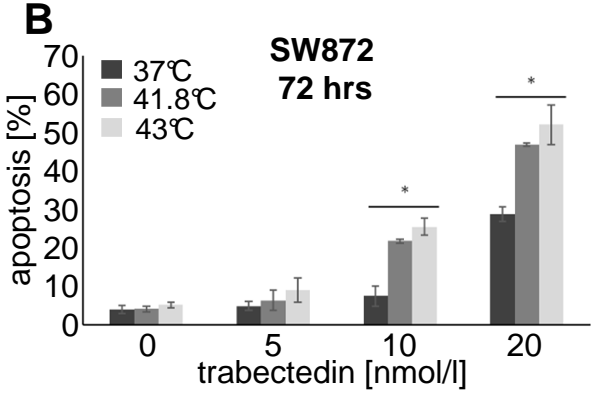
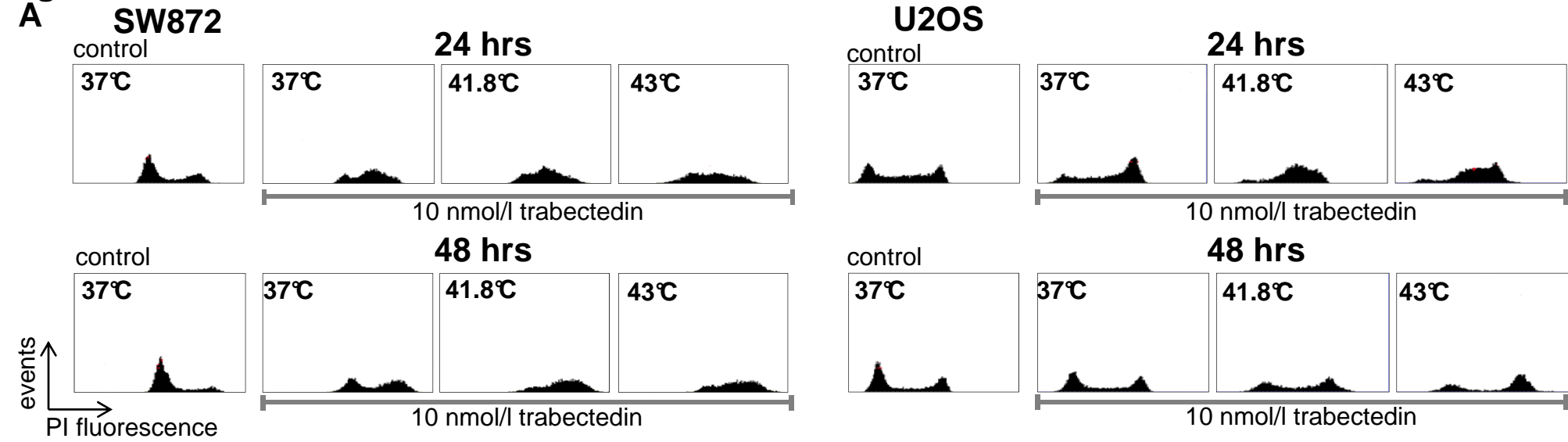
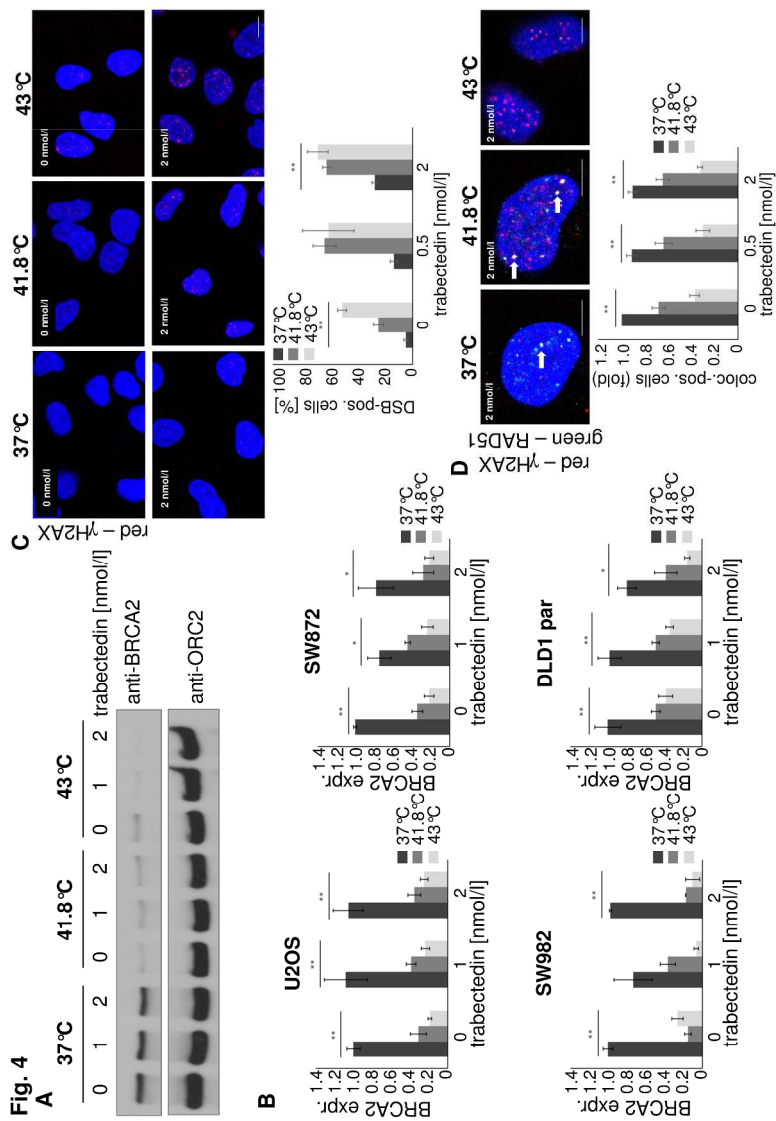
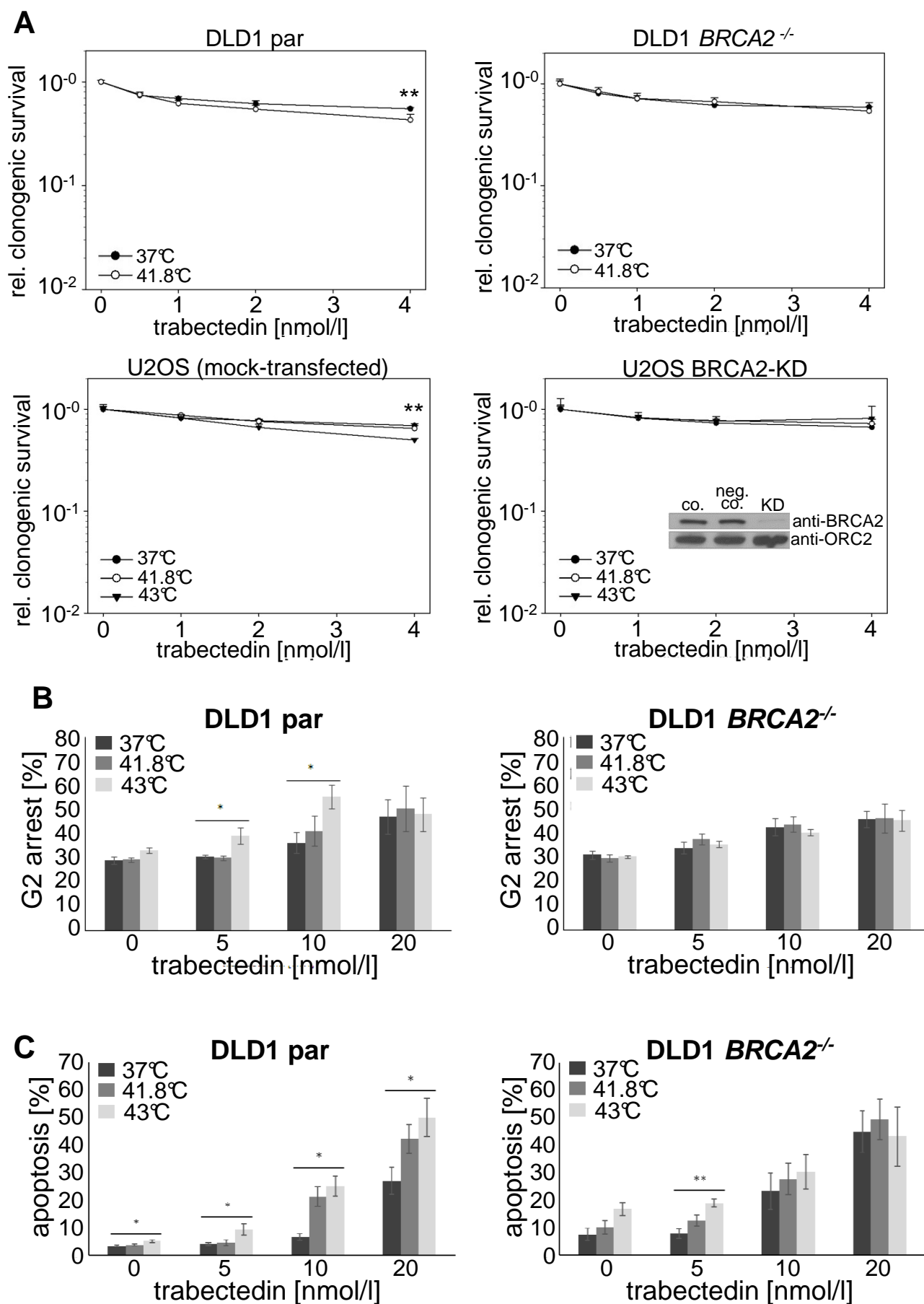
Fig. 2

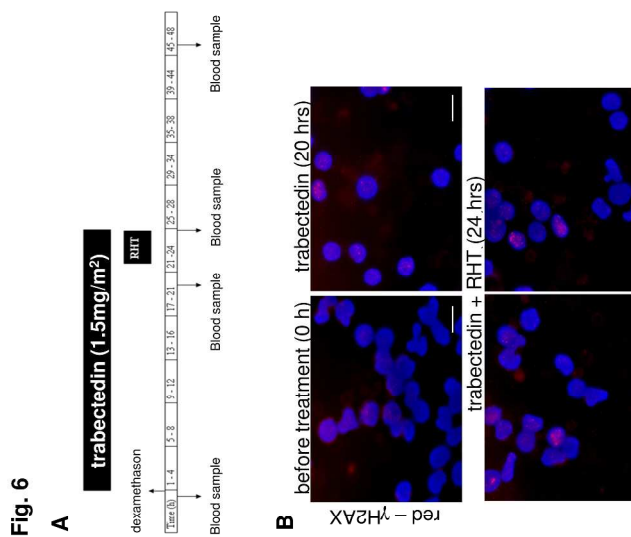
Fig. 3





297x420mm (300 x 300 DPI)

Fig. 5



297x420mm (300 x 300 DPI)

AC

Fig. S1

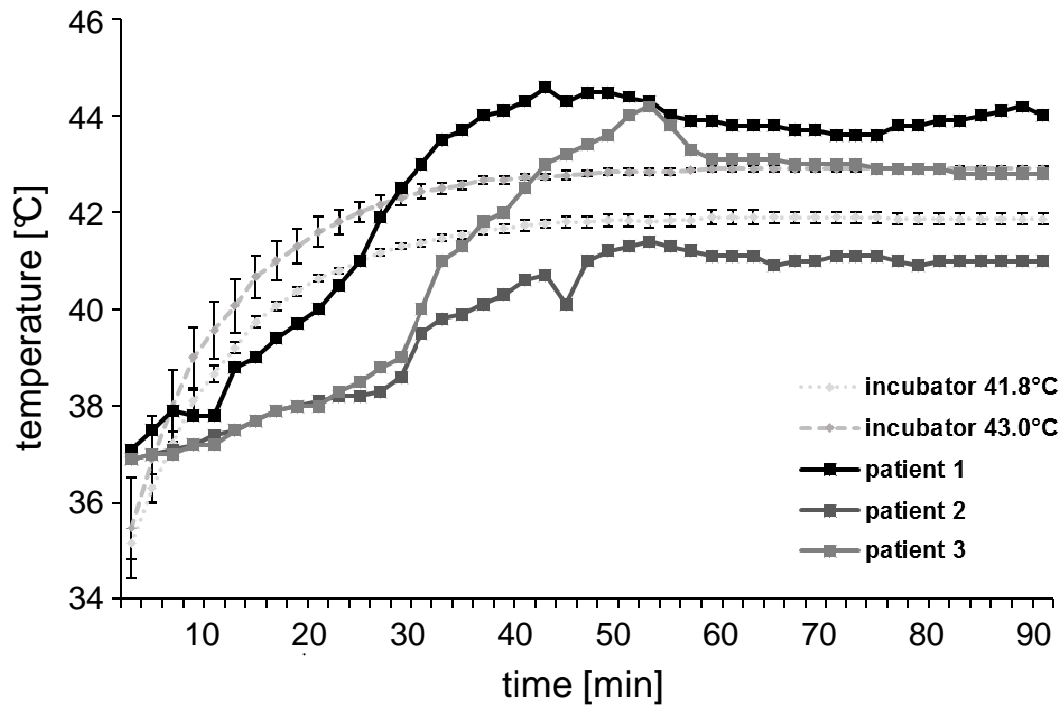
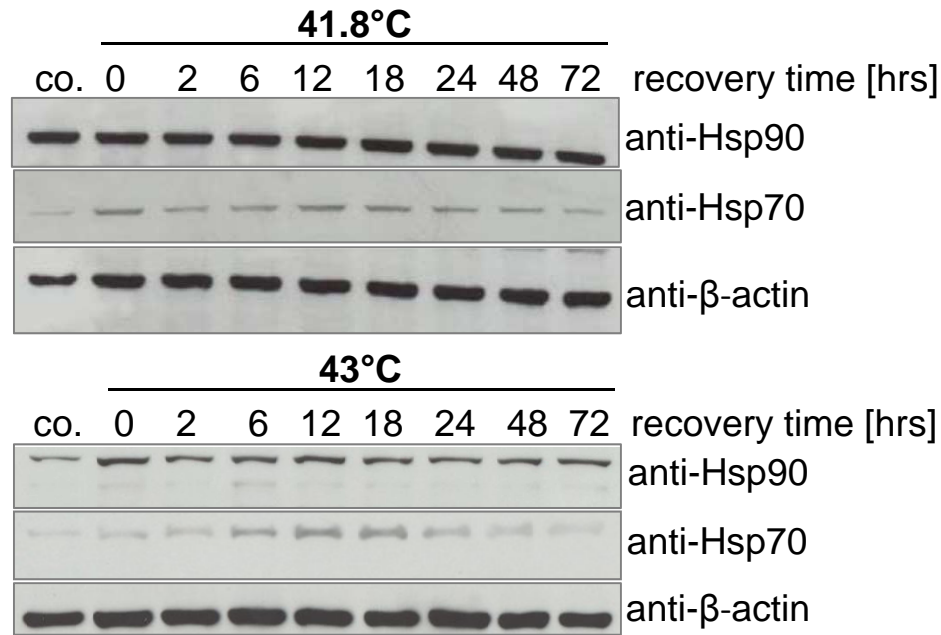
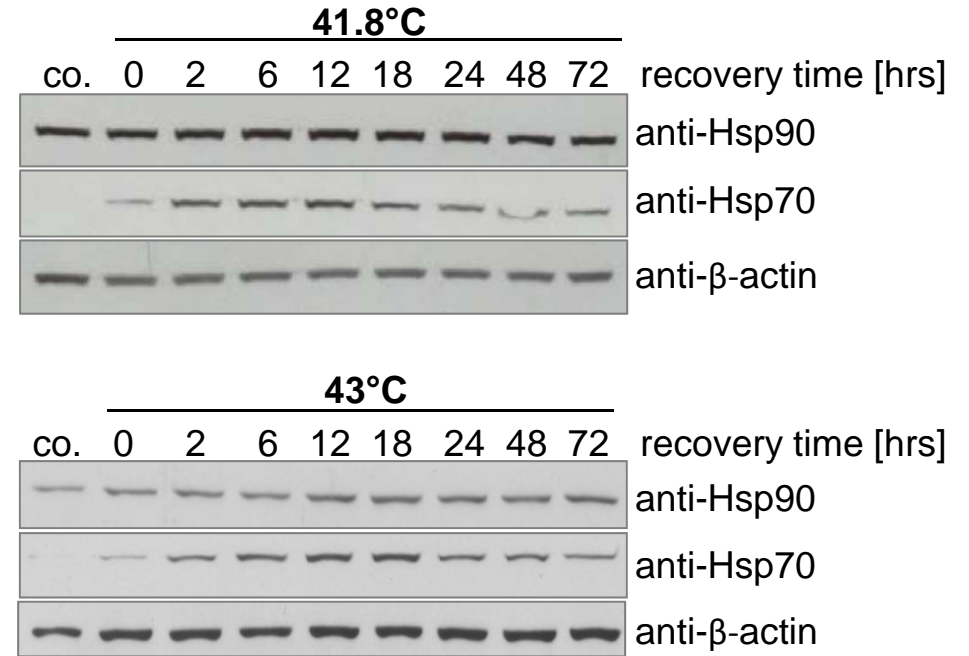


Fig. S2

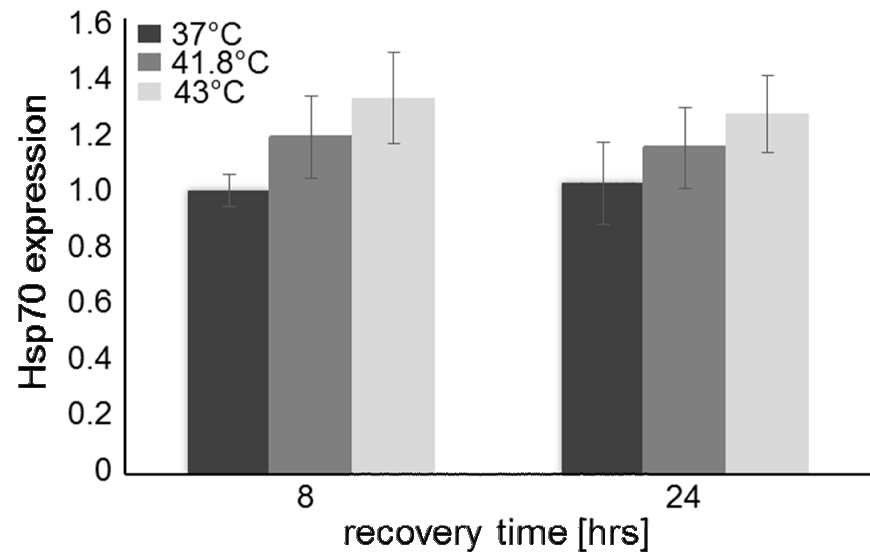
A SKUT-1



B SW872



C



D U2Os

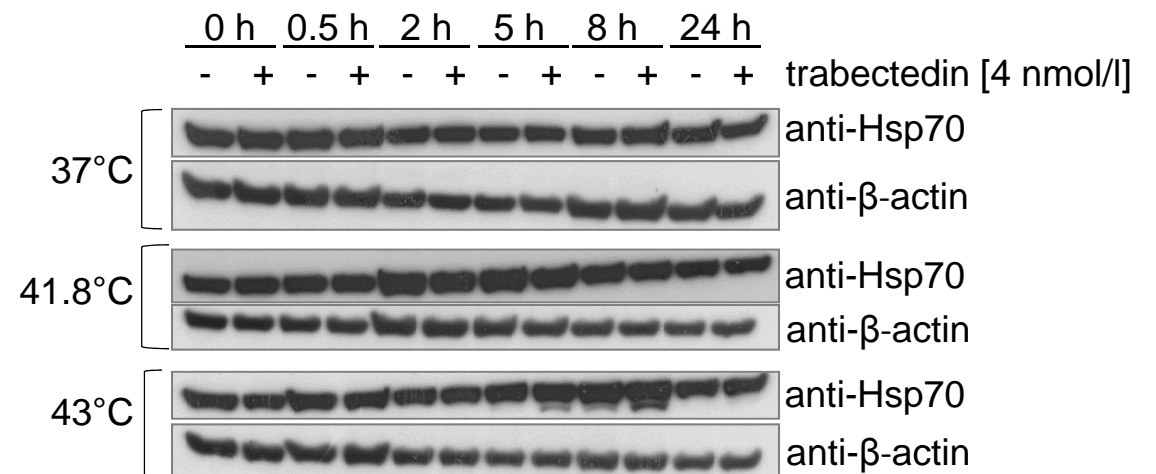
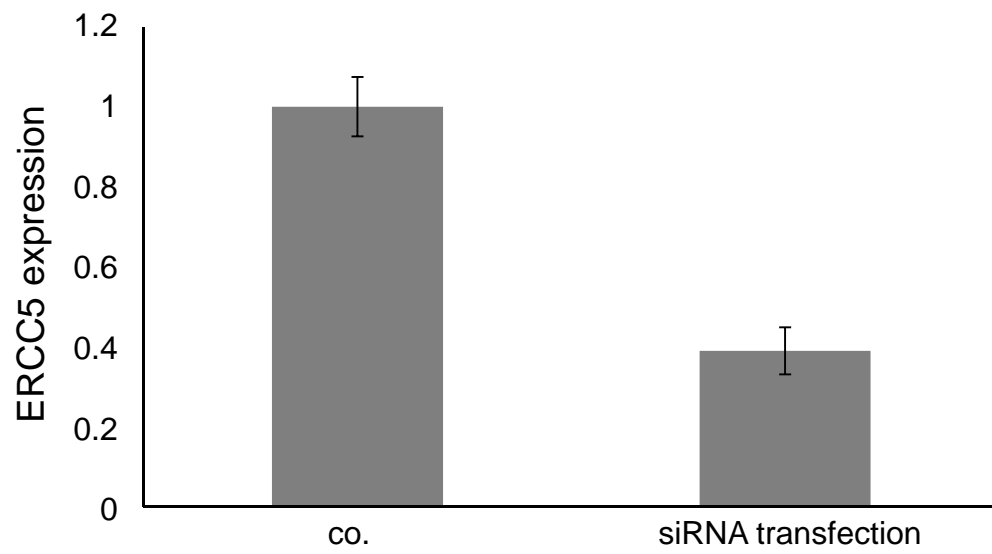


Fig. S3

Tab. S1

| Cell line | TP53 status | Reference |
|-----------|---------------|---|
| U2OS | wild type | Diller et. al., Mol Cell Biol 1990;10:5772–81 |
| SW872 | mutant | Ohnstad et al., Cancer 2013; 119:1013–22 |
| SW982 | not available | |
| SKUT-1 | mutant | Smardova et. al., Oncol Rep 2005;14:901-7 |
| RD-ES | mutant | Komuro et. al., Cancer Res 1993;53:5284-8 |
| DLD1 | mutant | Li et. al., Mol Cancer Ther 2005;4(6):901–9 |

Accepted